AIP Applied Physics Letters

Dramatically enhanced polarization in (001) , (101) , and (111) BiFeO 3 thin films due to epitiaxial-induced transitions

Jiefang Li, Junling Wang, M. Wuttig, R. Ramesh, Naigang Wang, B. Ruette, A. P. Pyatakov, A. K. Zvezdin, and D. Viehland

Citation: Applied Physics Letters **84**, 5261 (2004); doi: 10.1063/1.1764944
View online: http://dx.doi.org/10.1063/1.1764944
View Table of Contents: http://scitation.aip.org/content/aip/journal/apl/84/25?ver=pdfcov
Published by the AIP Publishing

Dramatically enhanced polarization in (001), (101), and (111) $BiFeO_3$ thin films due to epitiaxial-induced transitions

Jiefang Li
Department of Materials Science and Engineering, Virginia Tech, Blacksburg, Virginia 24061

Junling Wang, M. Wuttig, and R. Ramesh
Department of Materials and Nuclear Engineering, University of Maryland, College Park, Maryland 20742

Naigang Wang and B. Ruette
Department of Materials Science and Engineering, Virginia Tech, Blacksburg, Virginia 24061

A. P. Pyatakov and A. K. Zvezdin
Institute of General Physics, Russian Academy of Science, Vavilova St., 38, Moscow 119991, Russia

D. Viehland[a)]
Department of Materials Science and Engineering, Virginia Tech, Blacksburg, Virginia 24061

(Received 17 February 2004; accepted 3 May 2004; published online 10 June 2004)

Dramatically enhanced polarization has been found for (001), (101), and (111) films, relative to that of $BiFeO_3$ crystals. The easy axis of spontaneous polarization lies close to (111), for the various oriented films. $BiFeO_3$ films grown on (111) have a rhombohedral structure, identical to that of single crystals; whereas films grown on (101) or (001) are monoclinically distorted from the rhombohedral structure, due to the epitaxial constraint. © *2004 American Institute of Physics*. [DOI: 10.1063/1.1764944]

Ferromagnetoelectric materials have two order parameters.[1,2] These are a spontaneous polarization P_s and a spontaneous magnetization M_s. Of particular interest is $BiFeO_3$ (BF), which exhibits the coexistence of ferroelectric and antiferromagnetic (G-type) order up to quite high temperatures.[1] In bulk single crystals, $BiFeO_3$ has a ferroelectric Curie temperature T_C of 850 °C,[3,4] and an antiferromagnet Néel temperature T_N of 310 °C.[5,6] The lattice structure of $BiFeO_3$ crystals is a rhombohedrally distorted perovskite,[5,7–11] which belongs to the space group $R3c$ (or C_6^{3V}). The rhombohedral unit cell parameters are $a_r = 3.96$ Å and $\alpha_r = 0.6°$.

In this structure, the hexagonal $(001)_H$ is equivalent to the pseudocubic $(111)_c$, along which there is a three-fold rotation, and about which the Bi^{3+} and Fe^{3+} cations are displaced from their centro-symmetric positions. This distortion is polar and results in a P_s of 0.061 C/m^2 oriented along $(111)_c$. Along $(001)_H/(111)_c$, $BiFeO_3$ has antiferromagnetic order.[1,8] Microscopically, the antiferromagnetic spin order is not homogeneous[5,8,9]. An incommensurate spin cycloid with a long wavelength λ of ~600 Å[10–13] is present, which is oriented along $(110)_H$. The 3 m magnetic point group allows for a linear magnetoelectric effect α_E, but for $BiFeO_3$ the antiferromagnetic vector and linear magnetoelectric effect are both averaged to zero over λ.[14,15]

Recently, dramatically increased P_s and α_E have been reported in epitaxial thin films of $BiFeO_3$ grown on $(001)_c$ $SrTiO_3$.[16] For example, the P_s of (001) $BiFeO_3$ thin films is ~0.6 C/m^2—which is ~20× larger than that of a bulk crystal. Clearly, hetero-epitaxy induces significant and important structural changes. The lattice parameters, $(c,a) = (4.005, 3.935)$ Å, of thin films are not the rhombohedral ones of bulk single crystals and ceramics, ($a_r = 3.96$ Å). Recent electron spin resonance investigations of $BiFeO_3$ crystals under high-magnetic field H have shown an induced phase transition from cycloidal to homogeneous spin orders along $(111)_c/(001)_H$.[17] For variously oriented films, this letter shows that epitaxial constraint induces dramatic changes in ferroelectric polarization and in crystal lattice parameters.

We have grown phase-pure $BiFeO_3$ (BFO) thin films of 2000 Å thickness by pulsed laser deposition onto $(001)_c$,$(110)_c$, and $(111)_c$ single crystal $SrTiO_3$ substrates. The conducting perovskite oxide electrode, $SrRuO_3$ (SRO),[18]

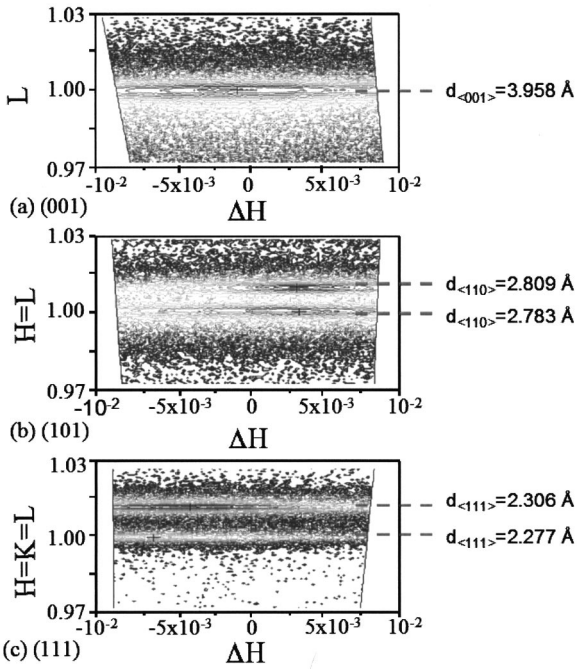

FIG. 1. Reciprocal space scans for $BiFeO_3$ single crystals taken about various zones about (001). (a) ($H0L$) zone; (b) (HHL) zone; and (c) (HHH) zone. The intensity is given on a log scale.

[a)]Electronic mail: dviehlan@vt.edu

TABLE I. Summary of interplanar spacing and lateral correlation lengths oriented from small area reciporcal lattice scans for the variously oriented $BiFeO_3$ films and crystal. Peak splitting was observed along the (101) and (111), the relative intensities are designated by *I*, and the weaker peak is designated by brackets.

Lattice spacing	Crystal	(111) film	(101) film	(001) film
$d_{\langle 001\rangle}$	3.958 Å	3.959 Å	3.984 Å	4.001 Å
$d_{\langle 101\rangle}$	2.783 Å(I=0.62)			2.792 Å(I=0.72)
	[2.809 Å(I=0.38)]	2.810 Å	2.828 Å	[2.816 Å(I=0.28)]
$d_{\langle 111\rangle}$	2.277 Å(I=0.87)	2.306 Å(I=1.00)	[2.278 Å(I=0.02)]	2.278 Å(I=0.90)
	[2.306 Å(I=0.13)]		2.307 Å(I=0.98)	[2.304 Å(I=0.10)]

was chosen as the bottom electrode due to the closest lattice mismatch with the BFO structure. Films of SRO of 500 Å were deposited at 600°C in an oxygen ambient of 100 mTorr; and followed by the BFO film, deposited at 670°C in an oxygen ambient of 200 mTorr at the growth rate of 0.7 Å/s. The $BiFeO_3$ film thicknesses were all close to 2000 Å, which is necessary to reduce the influence of film thickness,[16] if the out-of-plane lattice parameters are to be compared. Chemical analysis was carried out by SEM x-ray microanalysis, indicating a cation stoichiometry in the BFO films of ~1:1. Reciprocal lattice mapping was performed using a Phillips MPD system. Ferroelectric measurements were performed using a RT 6000 test system (Radiant Technologies).

Mesh scans that were taken about (001), (101), and (111) for a $BiFeO_3$ bulk single crystal are shown in Figs. 1(a)–1(c), respectively. A single peak was found along the (001), with $d_{\langle 001\rangle}$=3.958 Å. This is in agreement with previous reports of rhombohedral phase.[5,7–11] A peak splitting was found along the (101) with $d_{\langle 101\rangle}$=2.783 and 2.809 Å, and along the (111) with $d_{\langle 111\rangle}$=2.277 and 2.306 Å. The values of the interplanar spacing are summarized in Table I. These results evidence a polydomain rhombohedral state.

Mesh scan taken along (001), (101), and (111) are shown in Figs. 2(a)–2(c) for a (111) oriented $BiFeO_3$ thin film. Both a sharp peak from the $SrTiO_3$ substrate (illustrated by arrows) and a borad peak from the film (grey lines to guide eyes) can be seen in each figure. The values of (*HKL*) were determined by referencing to the interplanar spacings of the bulk single crystal ($d_{\langle 001\rangle}$=3.958 Å, $d_{\langle 101\rangle}$=2.809 Å, and $d_{\langle 111\rangle}$=2.306 Å). The (111) oriented $BiFeO_3$ films were found to grow epitaxially on (111) $SrTiO_3$ substrates with values of the interplanar spacing of $d_{\langle 001\rangle}$=3.959 Å, $d_{\langle 101\rangle}$=2.810 Å, and $d_{\langle 111\rangle}$=2.306 Å. These interplanar spacing are equal to those of the bulk single crystal, as can be seen by comparisons in Table I. Apparently, the (111) $BiFeO_3$ films are in a single domain state with a rhombohedral structure.

The lattice structure of the (101) and (001) oriented $BiFeO_3$ thin films was found to be monoclinically distorted from the rhombohedral one. Mesh scans taken about (001), (101), and (111) are shown in Figs. 2(d)–2(f) for (101) films, and Figs. 2(g)–2(i) for (001) films, respectively. The values of the interplanar spacings are summarized in Table I. For both the (101) and (001) films, the values of $d_{\langle 111\rangle}$ were equal to those of the rhombohedral phase, whereas $d_{\langle 101\rangle}$ and $d_{\langle 001\rangle}$ were split. The (101) film is nearly single domain with $d_{\langle 111\rangle}$=2.307 Å (relative intensity, RI=0.98) and $d_{\langle 101\rangle}$=2.828 Å (RI=0.02), whereas the (001) film had a peak splitting about (111) and (101), with the dominant variant having values of $d_{\langle 111\rangle}$=2.277(RI=0.9) Å and $d_{\langle 101\rangle}$=2.792 Å(RI=0.72). The value of $d_{\langle 111\rangle}$ is equal to that of one of the domain variants of the rehombohedral structure of the bulk crystal; whereas $d_{\langle 110\rangle}$ was notably different than that for the bulk single crystal. This splitting indicates domain formation, with two variants populated. For both (101) and (001) oriented films, pronounced deviations in the value of $d_{\langle 001\rangle}$ were found from that of the bulk rhombohedral lattice. The value of $d_{\langle 001\rangle}$ increased from 3.959 Å for the (111)

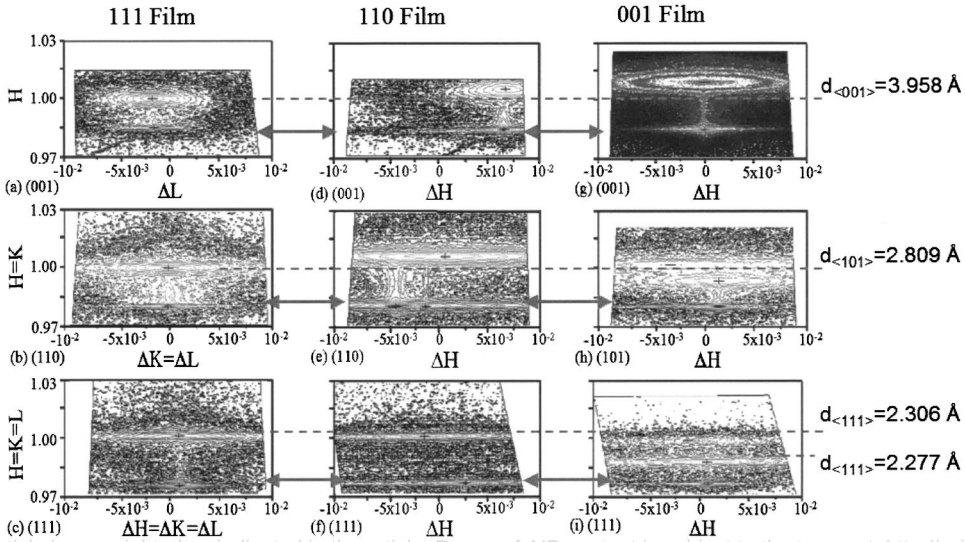

FIG. 2. Reciprocal lattice scans for various oriented $BiFeO_3$ films. (a) (001) scan for (111) film; (b) (101) scan for (111) film; (c) (111) scan for (111) film; (d) (001) scan for (101) film; (e) (101) scan for (101) film; (f) (111) scan for (101) film; (g) (001) scan for (001) film; (h) (101) scan for (001) film; and (i) (001) scan for (111) film. The values of (*HKL*) are normalized to those of $BiFeO_3$ single crystals, i.e., $(H,K,L)_{crystal}=(1,1,1)$. Intensity is given on a log scale. The grey arrows indicate the lattice parameters of the $SrTiO_3$ substrate.

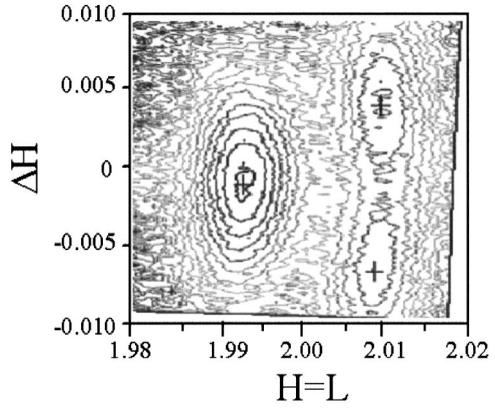

FIG. 3. (202) Mesh scans for a (001) oriented $BiFeO_3$ thin layer. The intensity lines on the contour maps are shown on a logarithmic scale. The values of (HKL) are normalized to those of $BiFeO_3$ single crystals, i.e., $(H,K,L)_{\text{crystal}} \equiv (1,1,1)$.

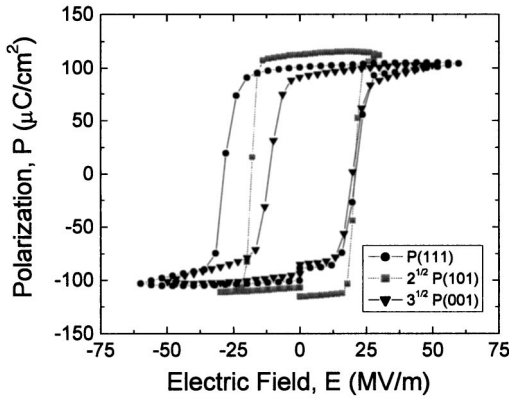

FIG. 4. P–E curve (001), (101), (111) $BiFeO_3$ films projected onto (111).

film, to 3.984 Å for the (101) film, to 4.001 Å for the (001) film.

A mesh scan about the *HLH* zone around (001) is shown in Fig. 3 for the (001) oriented $BiFeO_3$ thin layer. This contour scan was taken only along the film peaks, avoiding those of the substrate. The contour lines in Fig. 3 are given in a logarithmic scale. Three peaks can be scan consisting of (i) a splitting of *a* domains along (H00); and (ii) a splitting between *a* and *c* domains (*H*0*L*). These data give evidence that the stable phase of (001) oriented $BiFeO_3$ epitaxial thin layers is monoclinic. The monoclinic lattice parameters are $(a_m = b_m, c_m; \beta\text{-}90°) = (4.001\ \text{Å}, 3.935\ \text{Å}; 0.6°)$. This is the monoclinic M_a structure. It should be noted that the monoclinic angle β of the thin layer is nearly equal to that of the rhombohedral angle α of the bulk crystal. These results are preliminary to a further study of this film by synchrotron x-ray,[19] which is now being carried out.

On (111), $BiFeO_3$ films grow in an unconstrained single domain condition. The crystal structure is rhombohedral and identical to that of bulk crystals. Films grown on either (101) or (001) are under significant epitaxial constraint. The crystal structure is monoclinically distorted from the rhombohedral along the (001), as evidence by the values of $d_{\langle 001\rangle}$ in Table I. With respect to the rhombohedral lattice, the structure of (101) $BiFeO_3$ films expand along both (101) and (001); whereas that of (001) films contract along (101) and expand along (001).

We also investigated the effect of orientation of this constrained crystallographic film state on the physical properties of $BiFeO_3$. The ferroelectric properties were characterized by a polarization hysteresis method. For each orientation, we observed hysteresis loops typical of a ferroelectric. We found a remanent polarization P_r of $\sim 55\ \mu\text{C/cm}^2$ for (001) films, $\sim 80\ \mu\text{C/cm}^2$ for (101) films, and $\sim 100\ \mu\text{C/cm}^2$ for (111) films. Figure 4 shows $\sqrt{3}P_{(001)}$, $\sqrt{2}P_{(101)}$, and $P_{(111)}$ as a function of E for the variously oriented films. In this figure, the values of the projected polarizations can be seen to be nearly equivalent. This confirms that the direction of spontaneous polarization lies close to (111), and that the values measured along (101) and (001) are simply projections onto these orientations. Clearly, similar to bulk crystals and ceramics, the spontaneous polarization is oriented close to (111). However P_s is dramatically increased!

In summary, $BiFeO_3$ films grown on (111) have a rhombohedral structure, identical to that of single crystals, whereas films grown on (101) or (001) are monoclinically distorted from the rhombohedral by epitaxial constraint. The easy axis of spontenous polarization lies close to (111) for the variously oriented films.

The authors pleased to acknowledge support from the office of Naval Research (ONR) under Contract Nos. MURI N000140110761, N000140210340, N000140210126, NSF-MRSEC under Contract Nos. DMR-00-80008, and RFBR 01-02-1695. Input from Guangyong Xu and Gen Shirane concerning recent structural analysis of the $BiFeO_3$ films, cited in Ref. 19, is acknowledged.

[1] G. A. Smolenskii and I. Chupis, Sov. Phys. Usp. **25**, 475 (1982).
[2] E. K. H. Salje, Cambridge University Press, 1990.
[3] Yu. N. Venevtsev, G. Zhadanov, and S. Solov'ev, Sov. Phys. Crystallogr. **4**, 538 (1960).
[4] G. Smolenskii, V. Isupov, A. Agranovskaya, and N. Kranik, Sov. Phys. Solid State **2**, 2651 (1961).
[5] P. Fischer, M. Polomskya, I. Sosnowska, and M. Szymanksi, J. Phys. C **13**, 1931 (1980).
[6] G. Smolenskii, V. Yudin, E. Sher, and Yu. E. Stolypin, Sov. Phys. JETP **16**, 622 (1963).
[7] C. Michel, J.-M. Moreau, G. A. Achenbach, R. Gerson, and W. J. James, Solid State Commun. **7**, 701 (1969).
[8] J. D. Bucci, B. K. Robertson and W. J. James, J. Appl. Crystallogr. **5**, 187 (1972).
[9] J. R. Teague, R. Gerson, and W. J. James, Solid State Commun. **8**, 1073 (1970).
[10] Yu. E. Roginskaya, Yu. Ya. Tomashpol'skii, Yu. N. Venevtsev, V. M. Petrov, and G. S. Zhdanov, Sov. Phys. JETP **23**, 47 (1966).
[11] S. V. Kiselev, R. P. Ozerov, and G. S. Zhdanov, Sov. Phys. Dokl. **7**, 742 (1963).
[12] I. Sosnowska, T. Peterlin-Neumaier, and E. Steichele, J. Phys. C **15**, 4835 (1982).
[13] I. Sosnowska, M. Loewenhaupt, W. I. F. David, and R. Ibberson, Physica B **180–181**, 117 (1992).
[14] Yu. F. Popov, A. Zvezdin, G. Vorob'ev, A. Kadomtseva, V. Murashev, and D. Rakov, JETP Lett. **57**, 69 (1993).
[15] Yu. F. Popov, A. Kadomteseva, S. Krotov, D. Belov, G. Vorob'ev, P. Makhov, and A. Zvezdin, Low Temp. Phys. **27**, 478 (2001).
[16] J. Wang, J. Neaton, H. Zheng, V. Nagarajan, S. Ogale, B. Liu, D. Viehland, V. Vaithyanathan, D. Schlom, U. Waghamare, N. Spaldin, K. Rabe, M. Wuttig and R. Ramesh, Science **299**, 1719 (2003).
[17] B. Ruette, S. Zvyagin, A. Pyatakov, A. Bush, J. F. Li, V. Belotelov, A. Zvezdin, and D. Viehland, Phys. Rev. B **69**, 064114 (2004).
[18] C. Eom, R. J. Cava, R. Fleming, and J. Phillips, Science **258**, 1766 (1992).
[19] G. Xu and G. Shirane (private communication).